Electrochemical Observation of the Plasmonic Effect in Photochromic Ag Nanoparticle Filled Mesoporous TiO 2 Films

Nelly Couzon, Mathieu Maillard, Laurence Bois, Fernand Chassagneux, Arnaud Brioude

Electrochemical Observation of the Plasmonic Effect in Photochromic Ag Nanoparticle Filled Mesoporous TiO_2 Films

Nelly Couzon, Mathieu Maillard, Laurence Bois, Fernand Chassagneux, Arnaud Brioude.*

Laboratoire Multimatériaux et Interfaces, UMR CNRS 5615, Université Claude Bernard Lyon 1, France

ABSTRACT

We report photoelectrochemical measurements from mesoporous titanium dioxide filled with silver nanoparticles under illumination. A 200 mV potential switch of silver ion reduction is observed, depending on light wavelength. An easier reduction of silver in the presence of light is linked to plasmon induced charge separation (PICS). SEM and TEM analysis before and after photo-electrochemistry have also shown an electrochemical Ostwald ripening during continuous visible irradiation, with a growth of silver particles at the sample surface. The combined use of mesoporous structures and electrochemical characterization enabled to quantify the change in silver reactivity during PICS and emphasizes the role of plasmon in photochromism.

1. Introduction

Small particles have specific properties which differ from the bulk material. Metal nanoparticles (NPs) for instance, have numerous applications especially in catalysis and electro-catalysis[1,2], because of their fascinating chemical and physical properties. A critical factor is NP size, which impacts the surface-to-volume ratio, reactivity and efficiency in catalysis.[3] To understand the effect of size on NP properties, electrochemical techniques are particularly interesting.[4] Henglein[5] and Plieth[6] co-workers demonstrated that the standard redox potential of silver NPs decreases with decreasing size, making small particles more prone to oxidation. Experimentally, Brus et al[7] observed an electrochemical Ostwald ripening process of silver particle films on a conductive substrate. The growth of the largest particles at the expense of the smaller ones was attributed to a negative shift of the redox potential of smaller-sized particles. This was the first experimental observation confirming the prediction of Henglein & Plieth. Several other groups have worked on voltammetric behavior of silver nanoparticles. Ivanova's group[8] observed a negative shift of 100 mV of the silver NP potential when the size decreased from 40 to 10 nm. The surface coverage of metallic species and the substrate have also an significant impact on the position of the oxidation peak.[9–11]

In this paper, we focus on the electrochemical properties of silver NPs in a titanium oxide mesoporous layer. TiO_2 is one of the most studied semiconductors of our time[12–14] and its wide band gap energy (3-3.2eV) is a well-known problem as it mostly absorbs UV light corresponding to only 5% of the solar spectrum. To improve TiO_2 material, several methods are currently being studied. Among them, introducing mesoporosity is of great interest in increasing the interface with the electrolyte.[15–17] Mesoporosity provides a high surface area for reactive sites, and nanoscale channel walls facilitate transport of the photogenerated electron-hole pairs to the

surface, reducing the recombination rate into the bulk by increasing charge transfer.[18,19] Mesoporosity also allows a selective incorporation of various guest compounds inside the host framework or on the surface of the pore walls, resulting in a high host–guest interface with enhanced light absorption and photo-activity.[20,21] The synthesis by the Evaporation Induced Self-Assembly (EISA) process, first reported by Brinker's group [22–24], is among the easiest and most rapid methods for the preparation of mesoporous thin films.

Silver NPs are of particular interest for TiO_2 modification due to the plasmonic resonance of Ag NPs in the UV/visible range[25–27] and its remarkable photocatalytic activity.[28–31] Silver is also well-known for its photochemical activity. For example, light induces the formation of metallic silver seeds in a silver halide emulsion used in photography making silver reduction easier.[32–34] Adding TiO_2 to a silver NP environment induces drastic property changes. Interactions between silver and TiO_2 with light, lead in particular to photochromism properties[35–37]: silver NPs embedded in TiO_2 matrices become oxidized under visible light in air whereas oxidized species are reduced under UV-light exposure. The contact between Ag NPs and the semiconductor TiO_2 leads to a modification of Fermi level equilibration and to the formation of a Schottky barrier.[38] Depending on the irradiation, we expect to see several phenomena. Under visible light, excited plasmons from the Ag NPs create hot electrons with enough energy to cross the Schottky barrier.[29] Electrons are injected in the semiconductor conduction band allowing an electron-hole pair separation and an increased electronic conductivity.[39,40] This process is known as Plasmon Induced Charge Separation (PICS).[41] Under UV light, electrons are excited from the TiO_2 valence band (VB) to the conduction band (CB). Due to the lower Fermi level of metallic silver particles, photo-excited electrons are transferred from the TiO_2 CB to silver, creating an efficient charge separation.[42] The latter is called the co-catalysis effect.

In most studies concerning the electrochemical behavior of metallic NPs, the particles are dropped on the substrate rather than being embedded in a mesoporous layer. Development of mesoporous oxide layers using the block copolymer self-assembly method opened the way to fabrication of new electrodes.[43] Electrochemical studies of new electrodes consisting of metallic NPs embedded in a mesoporous oxide lead to a better understanding of metallic NP electrochemical behavior. The plasmonic effects play a central role and yet a mechanism description from an electrochemical point of view is relatively scarce. For this reason, we choose here to use electrochemistry measurements as a probe for the evolution of the silver NPs embedded in a TiO_2 mesoporous film, under the effect of light. If we consider the interaction with light, then metallic NPs interact with the surrounding electrolyte, mesoporous semiconductor TiO_2 substrate support and undergo a cycling potential, which could significantly modify the system.[9] Electrochemical studies are carried out to follow the impact of intermittent or continuous light irradiation on silver electrochemical behavior. Characterization of Ag-TiO_2 composite films before and after photo-electrochemical measurements by SEM/EDX and TEM allow the study of the effect of light on these silver-TiO_2 electrodes.

2. Experimental section

Materials

A polyethylene oxide-polypropylene oxide-polyethylene oxide block copolymer, Pluronic® P-123 ($(EO)_{20}$-$(PO)_{70}$-$(EO)_{20}$), tetraorthobutyltitanate ($Ti(OBu)_4$, TBT), silver nitrate ($AgNO_3$), formaldehyde (CH_2O) were all purchased from Sigma Aldrich and used as received. HCl 37%

was purchased from Carlo Erba. The FTO (Fluorine doped Tin Oxide) substrate (3x3 cm, 600 nm of FTO-deposited by CVD) was purchased from Solems.

Synthesis of Ag/TiO_2 films

Mesoporous TiO_2 films were synthesized using the Evaporation Induced Self Assembly (EISA) technique. During a typical synthesis, 1 g of Pluronic® P-123, used as structuring agent, is added to a solution of TBT (3.4 g), HCl (3.2 g) and EtOH (12 g). The molar ratio of Ti:H_2O: HCl is 1:11.2:3.22. Films are then deposited by a dip-coating method on FTO substrates, at 2 $mm.s^{-1}$. The films are aged under ambient conditions (T=23°C, RH=40-50%) for 24 h then calcinated at 400°C during 4 h, with a heating ramp of $1°C.min^{-1}$.

In order to form silver NPs inside the mesoporous titania film, an impregnation method is used. Briefly, an ammonia silver solution is prepared by adding ammonium hydroxide solution (25%) to a silver nitrate aqueous solution (50 mM), until a clear solution is obtained. The mesoporous films are immersed in this solution for 15 minutes. Then the silver ions are chemically reduced using formaldehyde. Films are immersed for 15 min at 80°C in a solution of 12 mM of formaldehyde in ethanol. The resulting films are washed with water and stored in a dark place at ambient condition. They are used within a month without noticeable variations.

For porosity measurements, TiO_2 powder was prepared using the same preparation method described above. The TiO_2 solution is heated at 50°C for 2 days then the solid is calcinated at 400°C for 2 h, with a heating ramp of $1°C.min^{-1}$.

Characterization

Scanning electron microscopy (SEM) images were obtained using a Zeiss Merlin Compact SEM with an in-lens detector at a low acceleration voltage of 5 kV. Energy dispersive X-ray analysis (EDX) was used to determine the amount of silver within the TiO_2 film. Transmission electron microscopy (TEM) was performed on a JEOL 2100F field emission instrument operating at 200 keV. In a typical procedure, TiO_2-Ag film fragments of non-controlled thickness were stripped off by scratching the samples with a razor blade and were then deposited on a carbon-coated copper grid. UV-Vis spectroscopy measurements were performed with a Safas UVmc spectrometer measuring absorbance from films under direct incidence. Scans were measured between 300 and 1000 nm, with a 2 nm resolution. Ellipsometric parameter measurements were performed with an atmospheric multi-wavelength Ellipso-Porosimeter EP-A SOPRA GES 5E. The effective indexes and thicknesses of layers constituting films were calculated using a modified Cauchy-type dispersive law. For porosity measurements, water vapor was condensed in the film, at a relative humidity (RH) varying from 0 to 98%. From the effective index at the chosen wavelength of 633 nm, the volume fraction of condensed water is calculated using the Lorentz-Lorenz law and is represented as a function of RH. The pore size distribution (PSD) is then obtained using the Kelvin relation.[44] Textural characterizations are realized using nitrogen adsorption/desorption isotherms on a BelsorpMini (Bel Instruments, Japan). Prior to analysis, samples were outgassed under vacuum (at 100°C for 4 h). Pore size distribution (max radius) and mesoporous volume were calculated from the adsorption branch of the isotherms using the Barrett-Joyner-Halenda (BJH) method. The total porous volume was measured at P/P_0 =0.98. The surface area was determined by the Brunauer-Emmett-Teller (BET) approach. The thickness of the films is measured using a Dektat profiler.

Photo-electrochemical (PEC) tests

All photo-electrochemical measurements were performed using a Volta lab PST006 Potentiostat with a three-electrode cell designed by Zahner Gmbh. A spiral Pt wire is used as the counter electrode and the reference electrode is a Re-5B Ag/AgCl electrode from BASi with a potential of 0.21V/NHE. The working electrode is our TiO_2-Ag film deposited on the FTO substrate (3x3 cm). The electrochemically active zone of the film is about 3.6 cm². For illumination tests, LED's of various wavelengths (360, 528, 660 nm or white light) were used. These LED were purchased from LED ENGINE Co. with a nominal flux of 120, 51, 260 and 91 mW/cm² respectively, at a working distance between the source and the sample of d=20 mm. Spectra from the sources and detailed measurements are provided in supplementary information S1.

Photocurrent measurements were carried out in a neutral electrolyte, Na_2SO_4 1M, at room temperature. During experiments, samples were irradiated from the back. A typical voltammetry cyclic experiment was performed with a potential sweep rate of 100 $mV.s^{-1}$ between -0.5 to +0.5 V during different time durations. After the electrochemical test, TiO_2-Ag films were rinsed with DI water and dried in air prior to further observations.

3. Results and discussion

Characterization of TiO_2-Ag film before PEC tests

Composite films are red/dark brown indicating that a large amount of silver NPs has formed inside the TiO_2 film. These colored samples were characterized by UV-Vis spectroscopy, and a typical spectrum is given in Figure 1. The spectrum in Figure 1 shows two main features. First,

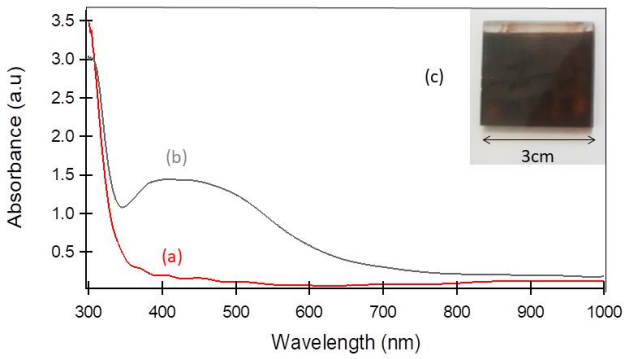

Figure 1: UV-Vis spectra of TiO_2 (a) and TiO_2-Ag (b) films and a photo of the TiO_2-Ag sample (c)

TiO_2 absorbs mostly in the UV-range (<350 nm), with or without the presence of silver NPs (Figures 1a and 1b). The larger TiO_2-Ag peak between 400 nm and 500 nm with a maximum at 420 nm is due to a surface plasmon resonance effect from silver NPs inside the TiO_2. This effect is greatly dependent on particle shape and size and also on the particle substrate.[45] Due to the high dielectric constant of TiO_2, a red-shift and broadening of the plasmon band is observed compared to what is usually observed for silver NPs in water or silica.[46] The peak width is attributed to a large size distribution of silver NPs.[47,48] This distribution can be observed in the following SEM and TEM images (see Figure 2a and b).

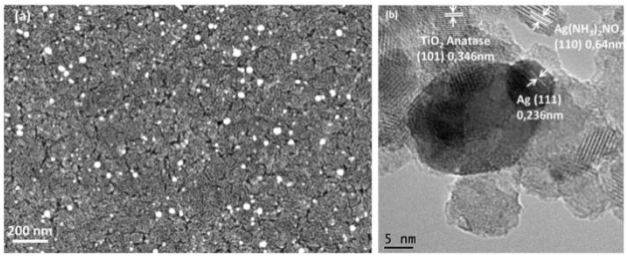

Figure 2: SEM (a) and TEM (b) images of TiO_2-Ag film

As can be seen from Figure 2a, the TiO_2 surface is a typical homogeneous worm-like mesoporous structure. Silver NPs, which are observed as white dots on the SEM image at the sample surface, have a large size distribution, from 7 to 40 nm, with an average size of 15 nm.

The EDS spectrum of TiO_2-Ag (Figure S2) shows 4 main peaks of Ti, O, Ag and Sn. The presence of Sn is due to the FTO substrate. A large amount of silver is present in the film, with a Ag:Ti atomic ratio of around 0.31.

The smallest silver NPs (<5 nm) can only be observed by TEM with the (111) lattice fringes at 0.236 nm (Figure 2b). This mostly corresponds to NPs present inside the TiO_2 mesoporous structure where the average NP diameter measured by TEM is 11 ± 5 nm. This is consistent with the SEM measurement. The TEM image also reveals the presence of $Ag(NH_3)_2NO_3$, a residual compound of silver impregnation, which possess characteristic large lattice interval around 0.64 nm, corresponding to a (110) lattice (fiche JCPDS n°01-076-1562). The TEM image also shows the presence of TiO_2 anatase, with the (101) lattice spacing at 0.346 nm.

The thickness was measured by the profiler and the average is 200 nm. Ellipsoporosimetry measurement confirmed this value and also showed that the TiO_2 film has a porous volume of about 24 %. Pore size was measured using the nitrogen adsorption technique (Figure S3) on TiO_2 powder and was about 9 nm, which is consistent with the NP size. With an atomic ratio of $Ag:TiO_2 = 0.31$ and a porous volume of 24 %, we can estimate that 70 % of the porosity is filled with metallic silver, based on the fact that silver is mostly located inside the pores. From the SEM picture on Figure 2 for example, we determined that the silver located on the surface represents only 0.7 % of total silver content, the remaining being in the 200 nm thick film. Details of this analysis are presented in supplementary information S4.

Photo-electrochemical study under alternate irradiation.

In a typical experiment, an I-V curve was obtained between -0.5 V to +0.5 V at a sweep rate potential of 100 $mV.s^{-1}$. These values were chosen in order to mainly observe the oxidation and reduction peaks of silver. In the first experiment, we used cycling with alternate irradiation and, as a result, observed a direct influence of light on the voltammetric behavior. Figure 3 shows a cyclic voltammogram from an alternation of cycles with and without white light irradiation. These voltammograms are given after the time necessary for the system to stabilize, corresponding to 50 cycles.

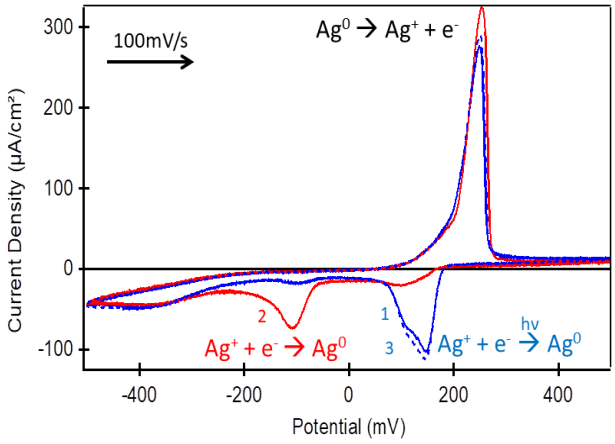

Figure 3: I-V curve of TiO_2-Ag with alternate irradiation: under white light (blue cycle n°1, blue dotted cycle 3) and without light (red, cycle n°2)

The I-V curve from TiO_2-Ag shows only one peak of silver oxidation around 250 mV. However, the interesting point concerns the Ag^+ reduction peaks. Figure 3 clearly shows that light has a direct impact on the reduction of silver ions produced during oxidation, as there is a large potential shift due to light exposure. In fact, under irradiation, the main reduction peak is around 140 mV, with a second smaller peak at -100 mV. However, without light, the opposite effect is observed, i.e. there is a main peak at around -100 mV and a second smaller peak around 110 mV. This shift is also present at the initial time (Figure S5) but not as well defined as after 50 cycles. An increase in the reduction current is also noted under light exposure. The

demonstration that potential switch is mostly due to light is the total reversibility of the effect: potential switch back to higher values when light is switched back on (from cycle 2 to 3), thus potential follows the light alternation.

The white light irradiation effect is also found with UV and other visible wavelengths i.e. at 360 nm and 528 nm, while an intermediate effect is obtained at 660 nm. Figure 4 presents the I-V curve of these different wavelengths.

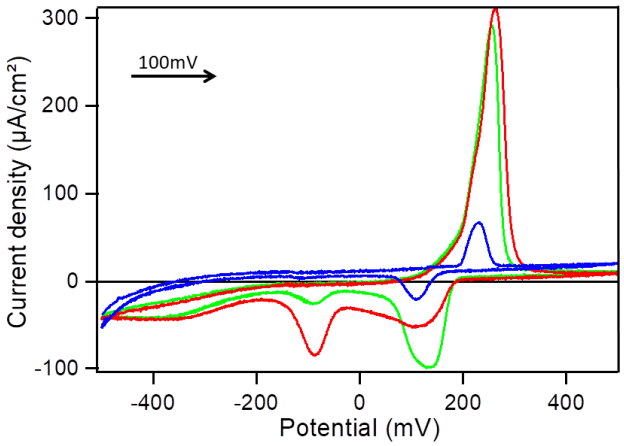

Figure 4: I-V curve of TiO_2-Ag electrode under 360nm (blue), 528 nm (green) and 660 nm (red) light

The oxidation peak is observed at the same potential regardless of the irradiation (±10 mV). On the other hand, the reduction peak clearly depends on irradiation wavelength. For example, at 660 nm, the main reduction peak appears around -100 mV and a second peak is also observed at 120 mV, which is similar to that observed without irradiation. On the other hand, when irradiated with UV or at 528 nm, the main reduction peak is shifted to approximately 130 mV. We can also note a slight shift of the reduction peak potential between UV and 528 nm light. With irradiation at 528 nm, the potential peak is around 140 mV whereas under UV light the peak is at 110 mV. In addition, the I-V curve obtained under green light still exhibits a residual reduction peak

around -100 mV, whereas under UV light, this peak is no longer observed. Lastly, a strong decrease in intensity is observed under UV light.

The above observations confirm that the silver electrochemical response in this titania support is very sensitive to the presence of visible and UV light. In this experiment, we observe an easier reduction of Ag^+ in the titania layer induced by light as can be seen from the shift in the reduction peak, from -100 mV to +120 mV. To explain this significant shift, we assume that silver NPs in the titania film follow a PICS process under visible light.[41,49,50] PICS occurs at the interface between a semiconductor and plasmonic metal NPs and it involves electron injection from the plasmonic NP to the semiconductor CB.[51] Electron accumulation inside the titania CB allows an increase in electronic conductivity of the TiO_2.[40] The process is similar to latent image in photography, wherein the Ag^+ reduction is easier due to irradiation.[33] In our cyclic voltammetry experiment, we observe this easier reduction as a shift of the reduction potential. On the other hand, the oxidation peak remains unchanged under light irradiation, presumably because the plasmon excited state is too short-lived to be observed using cyclic voltammetry.

Under UV light, two complementary phenomena are observed. First, a co-catalysis effect is seen. TiO_2 is excited, creating photo holes and electrons. In the initial stage, the Schottky barrier formed at the Ag-TiO_2 interface prevents electron transfer from the TiO_2 CB to the Ag NPs. Accumulation of electrons in the TiO_2 CB is accompanied by a negative shift of the CB potential, allowing an overflow of electrons from TiO_2 to Ag.[52] Reduction reactions then occur more easily at NP surface than at the semiconductor surface. Ag^+ reduction is facilitated on Ag NPs and a significant intensity decrease is then observed in the electrochemical curve (Figure 4). We also assume that under this UV light, some of the Ag NPs also become excited, as their absorption band is close to UV. The PICS process, as described under visible light, can also be

observed under UV light and creates a shift in the silver reduction potential. The above phenomena cannot be observed without irradiation as there is no electron accumulation inside TiO_2. For 660 nm irradiation, only a few silver NPs are excited, which leads to an intermediate effect in the electrochemistry data.

To prove this hypothesis, we performed another experiment, in which the TiO_2-Ag electrode is irradiated with white light for 10 minutes without any applied potential and then submitted to electrochemical cycling without irradiation during 10 cycles. The voltammetric results are shown in Figure 5.

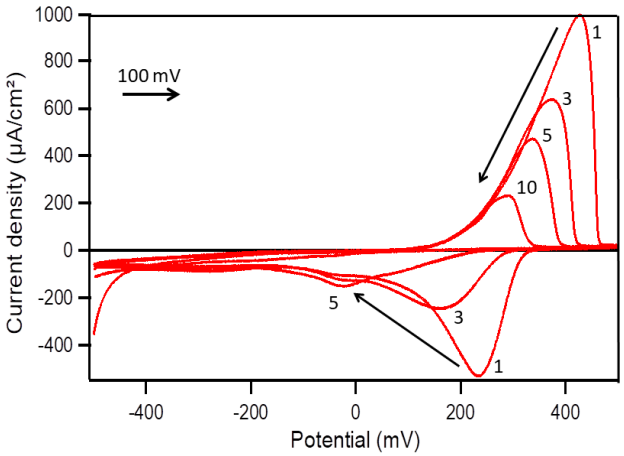

Figure 5: I-V curve for the TiO_2-Ag electrode after 10 min of white light irradiation

The oxidation peak is first observed at 400 mV but shifts rapidly to 300 mV. Two reduction peaks at 230 mV and -30 mV are observed initially, the one at higher potential corresponding to the highest current. This peak rapidly disappears, leaving a single reduction peak at -30 mV. This experiment, which is perfectly reproducible, is in agreement with the previous observation. In the presence of light, TiO_2-Ag electrode is modified by light-excited silver NPs, allowing an easier reduction of Ag^+ and a peak at higher potential can be observed during the first cycles. However, as electrochemical cycling is performed in the absence of light, the TiO_2-Ag electrode returns to

its ground state, leading to a reduction of Ag^+ at a lower potential, similar to experiments performed in the absence of light. These results clearly indicate that these electrodes are chemically modified by light, and can be probed even with an experimental time delay. Additionally, continuous decreases of both potential and intensity of cathodic and anodic peaks are observed. These decreases are linked to the diminution of the silver amount, due to a stripping of the silver nanoparticles.[10] Thus the shift of anodic potential peak shown here results mostly from the light-induced shift but also, on a longer time scale, from the silver loss.

Long term PEC study under continuous light irradiation

We study here the evolution of silver NPs in a mesoporous TiO_2 structure under the effect of both the electrochemical experiment and continuous light irradiation. The alternate experiment shows which process happens in the presence of light (UV or visible). This long term study is essential if we want to determine if silver NPs evolve due to irradiation and/or cyclic voltammetry. Thus, samples underwent 500 cycles between -0.5 and +0.5 V. Two types of irradiation were used: 360 nm (UV) and visible light. For comparison, an experiment was also carried out without irradiation. In Figure 6, we present three periods of cycling where the first five cycles show the "initial steps", cycles 50 to 55 show intermediate experiments and cycles from 495 to 500 present the long-term evolution.

Without irradiation:

The initial I-V curve of TiO_2-Ag without irradiation (Figure 6a) shows a typical oxidation and reduction peak of Ag^0 to Ag^+ and conversely. Oxidation occurs around 440 mV and the reduction peak is around 200 mV. Both the potential and intensity of these peaks evolves, with a

decrease in peak intensity and a shift to lower potentials, both being related to the progressive loss of silver and a size modification. We can note that the oxidation peak from the very first cycle always appears at a higher potential. During intermediate cycling (Figure 6b), the oxidation peak is mostly stabilized around 240 mV while the reduction peak mostly disappears and has completely shifted to -120 mV (inset Figure 6b). This large shift in reduction potential observed between initial and intermediate time is the same as that observed in Figure 5. In the absence of light, silver reduction becomes more difficult as no excited species are present to promote electronic transfer between TiO_2 and Ag NP. The initial higher reduction potential might be

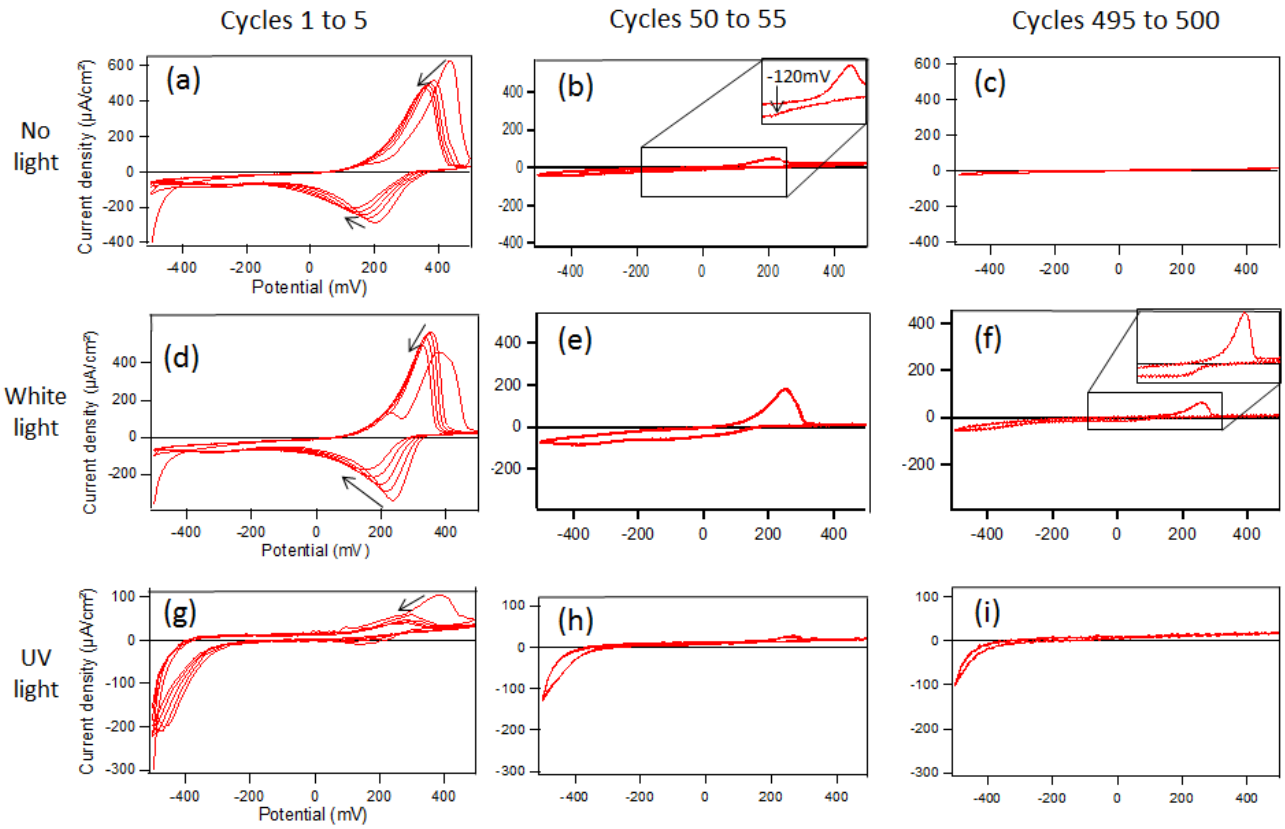

Figure 6: I-V curves of TiO_2-Ag without irradiation cycles 1-5: a, cycles 50-55: b, cycles 495-500: c; under white light cycles 1-5: d, cycles 50-55: e, cycles 495-500: f and under 360nm, cycles 1-5: g, cycles 50-55: h, cycles 495-500: i.

explained by sample exposure to natural light before starting the experiment. Moreover, the reduction current is considerably reduced, by a factor 10, compared to previous experiments in which irradiation was also alternated. This reduction limitation means that reduction of Ag^+ becomes unlikely since silver mostly disappeared from the FTO vicinity. This difficulty is clearly seen at the end of cycling (Figure 6c), where the redox signal from silver barely exists. Concerning the oxidation peak, a shift from 370 mV to 220 mV is observed during the entire experiment. This shift is less important than for the reduction peak, and is associated with a decrease in the size of the silver NPs and to Ag^+ species diffusion within the electrolyte. During electrochemical cycling, silver NPs are oxidized and Ag^+ is then reduced on seeds or larger particles. This phenomenon corresponds to an electrochemical Ostwald ripening driven by the size-dependent redox potential of the silver NPs, in good agreement with the literature.[5,8,10] NP size modification but also Ag^+ diffusion into the electrolyte are responsible for the charge decrease in the oxidation peak.

Light irradiation: White light

The I-V curves obtained under white light exposure are shown in Figures 6d to 6f. Initially, the voltammograms obtained with and without white light irradiation are similar, with only a slight shift in the reduction potential toward higher values when the sample is irradiated. In both cases, the oxidation and reduction peaks shift toward lower potentials during the first cycles. Conversely, differences are clearly visible after a long cycling (Figure 6f). The silver oxidation peak intensity slowly decreases and reaches a value of 65 $\mu A.cm^{-2}$ after 500 cycles under visible irradiation, while without irradiation, the oxidation peak current disappears after 500 cycles. The reduction peak also differs as without irradiation, the peak potential is centered around -120 mV

after 50 cycles and completely disappears within 500 cycles. However, under visible light, the reduction peak is still present after the same number of cycles at 50 mV. The difference between reduction peak positions is related to light influence, as already stated in previous experiments. White light induces excitation of silver NPs embedded in the titania and reduction of Ag^+ is consequently favored. Silver NP/TiO_2 photoexcitation maintains the system's reactivity up to 500 cycles.

Light irradiation: UV light

Under continuous UV irradiation, the system response to voltammetry is completely different, as presented in Figure 6g to 6i. The silver oxidation peak is initially observed at 400 mV but the current intensity quickly decreases and the overall signal is very weak from the 5th cycle. Concerning the reduction current, a peak is observed at +180 mV in the first cycle but this peak disappears after the 2nd cycle and no more silver reduction was observed during the rest of the experiment. After 500 cycles (Figure 6i), any sign of silver electro-activity is lost and only a small photocurrent of 20 $\mu A.cm^{-2}$ is observed due to TiO_2. The presence of TiO_2 is a key factor in this experiment, as silver is in contact with the photo-excited TiO_2. This means that silver is submitted to a permanent flow of photogenerated electrons. The presence of UV-excited TiO_2 around Ag induces a direct reduction of Ag^+ by transferring photo-excited electrons from the TiO_2 CB to Ag^+.[47] This phenomenon explains why no reduction peak is observed. It is worth pointing out that when performing alternate cycling over a long period of time, we do not observe the oxidation and reduction intensity decrease seen in continuous irradiation experiments. The alternate light study was done with a time break between each 10 cycles of

electrochemistry. We assume that this time-break between two cycle sequences used in the alternate irradiation experiment play a role in the preservation of the current intensity.

Characterization of TiO_2-Ag electrodes after EC cycling

After the PEC experiment under irradiation, the samples change color from brown to light yellow or colorless, indicating a change in size or shape of silver NPs, due to silver oxidation. The structure of the TiO_2-Ag electrode has been investigated by SEM and TEM and the images obtained confirm these changes (Figures 7 and 8).

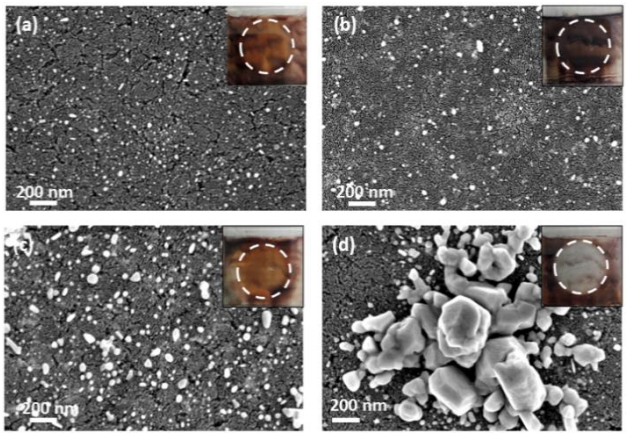

Figure 7: SEM images of TiO_2-Ag after electrochemistry under alternate light (a), without light (b), under 360nm (c) and under white light irradiation (d), and photo on inset (dashed line is the irradiated zone)

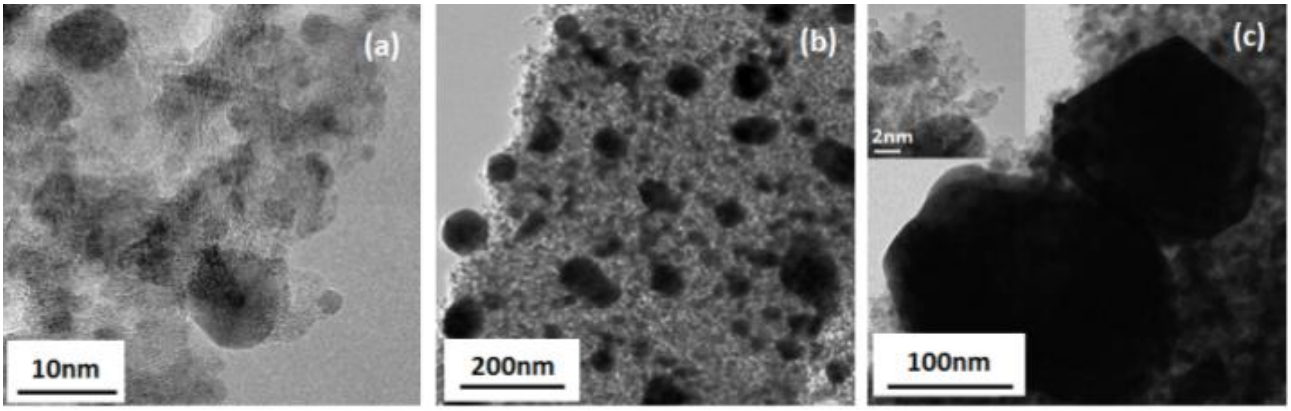

Figure 8: TEM images of TiO_2-Ag after electrochemistry without irradiation (a), under 360nm (b), and visible light (c) (inset: high magnification)

Experiments with alternate light lead to good film stability. In fact, after about 100 cycles with alternate irradiation, silver NPs only slowly evolve as observed by SEM (Figure 7a). The average size is 17 ± 7 nm, compared to 15 nm before electrochemistry. However, the amount of silver loss is about 17 % according to EDS measurements. We attributed this loss to the diffusion of silver ions within the electrolyte. The surface migration of silver NPs is low, with an atomic silver content on the surface of 1.1 % compared to 0.7 % before electrochemical experiments.

With continuous cycling without irradiation (Figure 7b), the size of the silver NPs on the surface only slightly changed from 15 ± 5 nm to 18 ± 10 nm after a 3h experiment, which corresponds to a moderate increase in size and size distribution due to migration to the sample surface. We quantified the silver located on the surface at approximately 0.7 % silver atomic content, which is the same than before any electrochemical experiment. Concerning silver loss, EDS measurement indicates a 15% loss compared to the initial state. Inside mesoporous TiO_2, the TEM images also show the presence of numerous silver NPs of 2 nm on average (Figure 8a).

Under continuous cycling with UV light, silver NPs on the surface (Figures 7c and 8b) grow from 15 nm ± 5 nm to 33 ± 20 nm. This is a manifestation of the well-known Ostwald ripening process.[7,53] The fact that silver particles mainly grow on the surface could be due to the presence of larger particles on the surface at the beginning of the experiment and also because growth is no longer confined by pore dimensions (≈10 nm). The diffusion process of silver in the electrolyte is here slowed down, with only a 10 % silver loss. Concerning surface migration, we estimate that 6 % of the silver atomic content is present on the surface after this experiment, so more than 10 times the quantity presents before the experiment.

Under continuous cycling with visible light, the electrode has completely lost its brown color (see inset in Figure 7d) and we observe the formation of silver aggregates of several hundreds of nanometers on the titania surface (Figures 7d & 8c). Similarly to experiments without light, there is still the presence of small NPs, with an average size of 2 nm, confirming electrochemical Ostwald ripening. A high silver loss is also observed, with almost 30 % loss according to EDS results. Surface migration has also been estimated at 13 % silver atomic content on the sample surface, which is visible on the SEM image. Visible light under a continuous electrochemical process clearly enhances electrochemical ripening and silver loss. Using alternate cycling under light allows this evolution to be slowed down.

These results are coherent with photochromism experiments under air where visible light irradiation induces discoloration by oxidation of the silver NPs within mesoporous TiO_2 matrix, whereas UV irradiation is able to restore coloration by reduction of Ag^+.[54] Photochromism is known to occur in the presence of oxygen as an oxidant. When used in an electrochemistry system, oxygen is no longer required and is replaced by the applied potential at the anode. A photochromism redox reaction is now divided in two distinct reactions occurring on both

electrodes at different times: first, silver oxidation occurring during positive overpotential and second, reduction during negative overpotential. To confirm the necessity of an applied potential in the photochromism mechanism, a sample was irradiated with white light, in the electrochemical cell with electrolyte, but without any electrochemical cycling. SEM images before and after irradiation show no difference, with a NP size remaining around 15 nm. Therefore, under our experimental conditions, the presence of TiO_2 does not induce any silver photo-oxidation and so, to explain electrode transformation, light, electrochemical cycling and titania are all necessary. It is suggested here that the rate of electrochemical ripening is increased by the action of visible light on silver in the presence of titania. The photochromic behavior of this silver/titania electrode is induced by electrochemical cycling,[37] the role of oxygen acceptor being replaced by electrical polarization. Electrode aging, which is manifested by discoloration, higher silver loss and formation of large aggregates at the surface, is much faster in the case of continuous cycling under visible or UV light. For practical application, silver loss could eventually be limited working below silver oxidizing potential or using a thin protective layer. The protective layer could be deposited using ALD for instance,[55] or partially oxidizing the silver core to form a silver oxide shell.[56]

We have schematized the global process in Scheme 1. During our PEC measurements, three steps can be dissociated: oxidation, diffusion and reduction. When experiments are done without irradiation (Scheme 1a), Ag^+ species are formed because of the applied potential. They can be reduced directly or can diffuse before reduction. Under white light (Scheme 1b), silver NPs absorb a large part of the visible light due to surface plasmonic resonance and thus creates a collective oscillation of electrons. Some of these electrons possess sufficient energy to overcome

the Schottky barrier and are injected into the TiO_2, leading to the formation of Ag^+ species, in addition to the ones created by the applied potential. The increased presence of Ag^+ species enhances the electrochemical Ostwald ripening process, with increase diffusion towards larger particles, creating large silver aggregates, as seen on the SEM image. The increased presence of charges also explains the shift in the silver reduction potential. Under UV light (Scheme 1c), photo-excited TiO_2 strongly promotes the formation of Ag(0) species due to photo-electron emission, in the same way decreasing the diffusion step. During the cyclic voltammetry measurement, this effect is seen by a significant intensity decrease of the redox peaks under alternate and continuous light (Figure 4 and 6g).

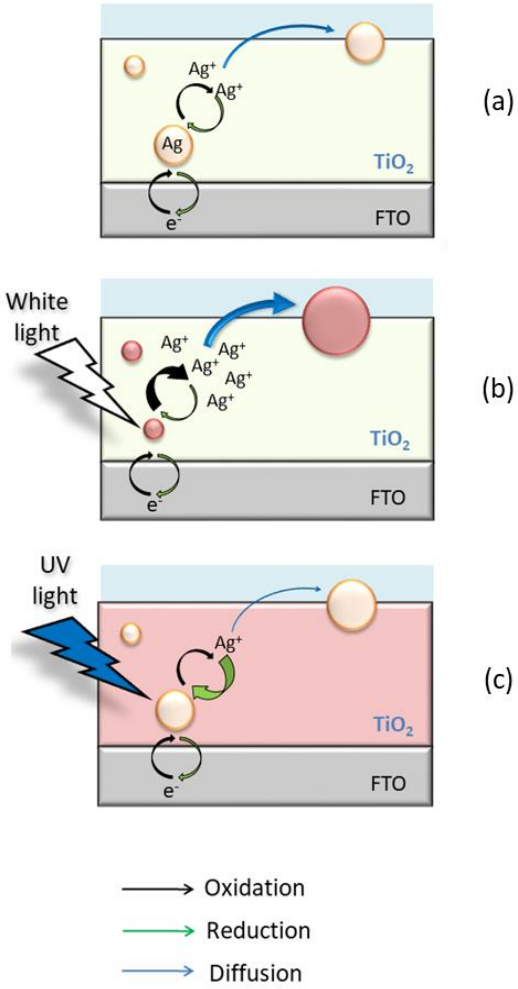

Scheme 1: Schematic of the oxidation diffusion reduction process without irradiation (a), under white light (b) and under UV light (c). Excited species are represented in red.

Conclusion

To conclude, we observed the electrochemical behavior of an electrode constituted of silver NPs embedded in a mesoporous TiO_2 film, under different light irradiation conditions. Experiments performed under alternate light revealed that the process of Ag^+ reduction inside a mesoporous titania support can be highly sensitive to light. The reduction potential of silver ions is increased by more than 200 mV with light exposure. Silver electro-reduction in a titania

support is modulated by plasmon-enhanced electron transfer between the titania and silver NPs. Silver electro-activity also depends on the wavelength of this light, and so experiments performed under a continuous UV light reveal that silver is maintained in a reduced form, under the control of photo-excited TiO_2. This trend in electrochemical behavior of the silver species inside titania is a manifestation of photochromism and confirms the influence of light on silver NPs embedded in titania.

Long-term cycling experiments performed under continuous visible light reveals a decrease in both oxidation and reduction currents. The electrode is progressively transformed due to electrochemical Oswald ripening, inducing the disappearance of the silver NPs and the formation of very large silver aggregates at the electrode surface. This process is enhanced via a photoelectrochromic process. The rate of this irreversible transformation is reduced using alternate light exposure.

ASSOCIATED CONTENT

Supporting Information. S1 Spectra and intensity of LEDs sources; S2 EDS spectrum of TiO_2-Ag film; S3 Nitrogen adsorption/desorption isotherm; S4 Silver surface estimation; S5 Initial alternate irradiation voltammetry

AUTHOR INFORMATION

Corresponding Author

* Phone: +33 4 72 43 16 08, e-mail : mathieu.maillard@univ-lyon1.fr

Author Contributions

The manuscript was written through contributions of all authors. All authors have given approval to the final version of the manuscript.

ACKNOWLEGEMENT

Funding Sources

This work was supported by the LABEX iMUST (ANR-10-LABX-0064) of the Université de Lyon, within the program "Investissements d'Avenir" (ANR-11-IDEX-0007) by the French National Research Agency (ANR).

REFERENCES

(1) Koper, M. T. M. Structure Sensitivity and Nanoscale Effects in Electrocatalysis. *Nanoscale* **2011**, *3*, 2054.

(2) Wu, B.; Zheng, N. Surface and Interface Control of Noble Metal Nanocrystals for Catalytic and Electrocatalytic Applications. *Nano Today* **2013**, *8*, 168–197.

(3) Masitas, R. A.; Khachian, I. V.; Bill, B. L.; Zamborini, F. P. Effect of Surface Charge and Electrode Material on the Size-Dependent Oxidation of Surface-Attached Metal Nanoparticles. *Langmuir* **2014**, *30*, 13075–13084.

(4) Kleijn, S. E. F.; Lai, S. C. S.; Koper, M. T. M.; Unwin, P. R. Electrochemistry of Nanoparticles. *Angew. Chem. Int. Ed.* **2014**, *53*, 3558–3586.

(5) Henglein, A. Small-Particle Research: Physicochemical Properties of Extremely Small Colloidal Metal and Semiconductor Particles. *Chem. Rev.* **1989**, *89*, 1861–1873.

(6) Plieth, W. J. Electrochemical Properties of Small Clusters of Metal Atoms and Their Role in the Surface Enhanced Raman Scattering. *J. Phys. Chem.* **1982**, *86*, 3166–3170.

(7) Redmond, P. L.; Hallock, A. J.; Brus, L. E. Electrochemical Ostwald Ripening of Colloidal Ag Particles on Conductive Substrates. *Nano Lett.* **2005**, *5*, 131–135.

(8) Ivanova, O. S.; Zamborini, F. P. Size-Dependent Electrochemical Oxidation of Silver Nanoparticles. *J. Am. Chem. Soc.* **2010**, *132*, 70–72.

(9) Toh, H. S.; Batchelor-McAuley, C.; Tschulik, K.; Uhlemann, M.; Crossley, A.; Compton, R. G. The Anodic Stripping Voltammetry of Nanoparticles: Electrochemical Evidence for the Surface Agglomeration of Silver Nanoparticles. *Nanoscale* **2013**, *5*, 4884.

(10) Brainina, K. Z.; Galperin, L. G.; Kiryuhina, T. Y.; Galperin, A. L.; Stozhko, N. Y.; Murzakaev, A. M.; Timoshenkova, O. R. Silver Nanoparticles Electrooxidation: Theory and Experiment. *J. Solid State Electrochem.* **2012**, *16*, 2365–2372.

(11) Brainina, K. Z.; Galperin, L. G.; Vikulova, E. V. Electrochemistry of Metal Nanoparticles: The Effect of Substrate. *J. Solid State Electrochem.* **2012**, *16*, 2357–2363.

(12) Fujishima, A.; Honda, K. Electrochemical Photolysis of Water at a Semiconductor Electrode. *Nature* **1972**, *238*, 37–38.

(13) Fattakhova-Rohlfing, D.; Zaleska, A.; Bein, T. Three-Dimensional Titanium Dioxide Nanomaterials. *Chem. Rev.* **2014**, *114*, 9487–9558.

(14) Fujishima, A.; Zhang, X.; Tryk, D. TiO_2 Photocatalysis and Related Surface Phenomena. *Surf. Sci. Rep.* **2008**, *63*, 515–582.

(15) Li, W.; Wu, Z.; Wang, J.; Elzatahry, A. A.; Zhao, D. A Perspective on Mesoporous TiO_2 Materials. *Chem. Mater.* **2014**, *26*, 287–298.

(16) Crepaldi, E. L.; Soler-Illia, G. J. de A. A.; Grosso, D.; Cagnol, F.; Ribot, F.; Sanchez, C. Controlled Formation of Highly Organized Mesoporous Titania Thin Films: From Mesostructured Hybrids to Mesoporous Nanoanatase TiO_2. *J. Am. Chem. Soc.* **2003**, *125*, 9770–9786.

(17) Grosso, D.; Cagnol, F.; Soler-Illia, G. J. de A. A.; Crepaldi, E. L.; Amenitsch, H.; Brunet-Bruneau, A.; Bourgeois, A.; Sanchez, C. Fundamentals of Mesostructuring Through Evaporation-Induced Self-Assembly. *Adv. Funct. Mater.* **2004**, *14*, 309–322.

(18) Abdolahi Sadatlu, M. A.; Mozaffari, N. Synthesis of Mesoporous TiO_2 Structures through P123 Copolymer as the Structural Directing Agent and Assessment of Their Performance in Dye-Sensitized Solar Cells. *Sol. Energy* **2016**, *133*, 24–34.

(19) Zhang, Y.; Xie, Z.; Wang, J. Supramolecular-Templated Thick Mesoporous Titania Films for Dye-Sensitized Solar Cells: Effect of Morphology on Performance. *ACS Appl. Mater. Interfaces* **2009**, *1*, 2789–2795.

(20) Liu, Z.; Li, Y.; Zhao, Z.; Cui, Y.; Hara, K.; Miyauchi, M. Block Copolymer Templated Nanoporous TiO_2 for Quantum-Dot-Sensitized Solar Cells. *J Mater Chem* **2010**, *20*, 492–497.

(21) Feng, D.; Luo, W.; Zhang, J.; Xu, M.; Zhang, R.; Wu, H.; Lv, Y.; Asiri, A. M.; Khan, S. B.; Rahman, M. M.; et al. Multi-Layered Mesoporous TiO_2 Thin Films with Large Pores and Highly Crystalline Frameworks for Efficient Photoelectrochemical Conversion. *J Mater Chem A* **2013**, *1*, 1591–1599.

(22) Brinker, C. J.; Lu, Y.; Sellinger, A.; Fan, H.; others. Evaporation-Induced Self-Assembly: Nanostructures Made Easy. *Adv. Mater.* **1999**, *11*, 579–585.

(23) Yang, H.; Coombs, N.; Dag, Ö.; Sokolov, I.; Ozin, G. A. Free-Standing Mesoporous Silica Films; Morphogenesis of Channel And Surface Patterns. *J. Mater. Chem.* **1997**, *7*, 1755–1761.

(24) Mahoney, L.; Koodali, R. Versatility of Evaporation-Induced Self-Assembly (EISA) Method for Preparation of Mesoporous TiO_2 for Energy and Environmental Applications. *Materials* **2014**, *7*, 2697–2746.

(25) Garmaroudi, Z. A.; Mohammadi, M. R. Plasmonic Effects of Infiltrated Silver Nanoparticles Inside TiO_2 Film: Enhanced Photovoltaic Performance in DSSCs. *J. Am. Ceram. Soc.* **2016**, *99*, 167–173.

(26) Rycenga, M.; Cobley, C. M.; Zeng, J.; Li, W.; Moran, C. H.; Zhang, Q.; Qin, D.; Xia, Y. Controlling the Synthesis and Assembly of Silver Nanostructures for Plasmonic Applications. *Chem. Rev.* **2011**, *111*, 3669–3712.

(27) Awazu, K.; Fujimaki, M.; Rockstuhl, C.; Tominaga, J.; Murakami, H.; Ohki, Y.; Yoshida, N.; Watanabe, T. A Plasmonic Photocatalyst Consisting of Silver Nanoparticles Embedded in Titanium Dioxide. *J. Am. Chem. Soc.* **2008**, *130*, 1676–1680.

(28) Zhou, W.; Li, T.; Wang, J.; Qu, Y.; Pan, K.; Xie, Y.; Tian, G.; Wang, L.; Ren, Z.; Jiang, B.; et al. Composites of Small Ag Clusters Confined in the Channels of Well-Ordered Mesoporous Anatase TiO_2 and Their Excellent Solar-Light-Driven Photocatalytic Performance. *Nano Res.* **2014**, *7*, 731–742.

(29) Liu, T.; Li, B.; Hao, Y.; Han, F.; Zhang, L.; Hu, L. A General Method to Diverse Silver/Mesoporous–metal–oxide Nanocomposites with Plasmon-Enhanced Photocatalytic Activity. *Appl. Catal. B Environ.* **2015**, *165*, 378–388.

(30) Albiter, E.; Valenzuela, M. A.; Alfaro, S.; Valverde-Aguilar, G.; Martínez-Pallares, F. M. Photocatalytic Deposition of Ag Nanoparticles on TiO_2: Metal Precursor Effect on the Structural and Photoactivity Properties. *J. Saudi Chem. Soc.* **2015**, *19*, 563–573.

(31) Abd-Elaal, A.; Parrino, F.; Ciriminna, R.; Loddo, V.; Palmisano, L.; Pagliaro, M. Alcohol-Selective Oxidation in Water under Mild Conditions via a Novel Approach to Hybrid Composite Photocatalysts. *ChemistryOpen* **2015**, *4*, 779–785.

(32) Schürch, D.; Currao, A.; Sarkar, S.; Hodes, G.; Calzaferri, G. The Silver Chloride Photoanode in Photoelectrochemical Water Splitting. *J. Phys. Chem. B* **2002**, *106*, 12764–12775.

(33) Tani, T. Physics of the Photographic Latent Image. *Phys. Today* **1989**, *42*, 36–41.

(34) Belloni, J.; Treguer, M.; Remita, H.; De Keyzer, R. Enhanced Yield of Photoinduced Electrons in Doped Silver Halide Crystals. *Nature* **1999**, *402*, 865–867.

(35) Bois, L.; Chassagneux, F.; Battie, Y.; Bessueille, F.; Mollet, L.; Parola, S.; Destouches, N.; Toulhoat, N.; Moncoffre, N. Chemical Growth and Photochromism of Silver Nanoparticles into a Mesoporous Titania Template. *Langmuir* **2010**, *26*, 1199–1206.

(36) Ohko, Y.; Tatsuma, T.; Fujii, T.; Naoi, K.; Niwa, C.; Kubota, Y.; Fujishima, A. Multicolour Photochromism of TiO_2 Films Loaded with Silver Nanoparticles. *Nat. Mater.* **2003**, *2*, 29–31.

(37) Tatsuma, T.; Suzuki, K. Photoelectrochromic Cell with a Ag–TiO_2 Nanocomposite: Concepts of Drawing and Display Modes. *Electrochem. Commun.* **2007**, *9*, 574–576.

(38) Kumar, M. K.; Krishnamoorthy, S.; Tan, L. K.; Chiam, S. Y.; Tripathy, S.; Gao, H. Field Effects in Plasmonic Photocatalyst by Precise SiO_2 Thickness Control Using Atomic Layer Deposition. *ACS Catal.* **2011**, *1*, 300–308.

(39) Cushing, S. K.; Li, J.; Meng, F.; Senty, T. R.; Suri, S.; Zhi, M.; Li, M.; Bristow, A. D.; Wu, N. Photocatalytic Activity Enhanced by Plasmonic Resonant Energy Transfer from Metal to Semiconductor. *J. Am. Chem. Soc.* **2012**, *134*, 15033–15041.

(40) Mubeen, S.; Hernandez-Sosa, G.; Moses, D.; Lee, J.; Moskovits, M. Plasmonic Photosensitization of a Wide Band Gap Semiconductor: Converting Plasmons to Charge Carriers. *Nano Lett.* **2011**, *11*, 5548–5552.

(41) Tatsuma, T.; Nishi, H.; Ishida, T. Plasmon-Induced Charge Separation: Chemistry and Wide Applications. *Chem Sci* **2017**, *8*, 3325–3337.

(42) Herrmann, J.-M.; Tahiri, H.; Ait-Ichou, Y.; Lassaletta, G.; Gonzalez-Elipe, A. R.; Fernandez, A. Characterization and Photocatalytic Activity in Aqueous Medium of TiO_2 and Ag-TiO_2 Coatings on Quartz. *Appl. Catal. B Environ.* **1997**, *13*, 219–228.

(43) Walcarius, A. Mesoporous Materials and Electrochemistry. *Chem. Soc. Rev.* **2013**, *42*, 4098–4140.

(44) Boissiere, C.; Grosso, D.; Lepoutre, S.; Nicole, L.; Bruneau, A. B.; Sanchez, C. Porosity and Mechanical Properties of Mesoporous Thin Films Assessed by Environmental Ellipsometric Porosimetry. *Langmuir* **2005**, *21*, 12362–12371.

(45) Diesen, V.; Dunnill, C. W.; Österberg, E.; Parkin, I. P.; Jonsson, M. Silver Enhanced TiO_2 Thin Films: Photocatalytic Characterization Using Aqueous Solutions of Tris(Hydroxymethyl)Aminomethane. *Dalton Trans* **2014**, *43*, 344–351.

(46) Hirakawa, T.; Kamat, P. V. Charge Separation and Catalytic Activity of Ag@TiO_2 Core−Shell Composite Clusters under UV−Irradiation. *J. Am. Chem. Soc.* **2005**, *127*, 3928–3934.

(47) Tobaldi, D. M.; Leonardi, S. G.; Pullar, R. C.; Seabra, M. P.; Neri, G.; Labrincha, J. A. Sensing Properties and Photochromism of Ag–TiO_2 Nano-Heterostructures. *J Mater Chem A* **2016**, *4*, 9600–9613.

(48) Okumu, J.; Dahmen, C.; Sprafke, A. N.; Luysberg, M.; von Plessen, G.; Wuttig, M. Photochromic Silver Nanoparticles Fabricated by Sputter Deposition. *J. Appl. Phys.* **2005**, *97*, 094305.

(49) Tian, Y.; Tatsuma, T. Plasmon-Induced Photoelectrochemistry at Metal Nanoparticles Supported on Nanoporous TiO_2. *Chem. Commun.* **2004**, No. 16, 1810.

(50) Tian, Y.; Tatsuma, T. Mechanisms and Applications of Plasmon-Induced Charge Separation at TiO_2 Films Loaded with Gold Nanoparticles. *J. Am. Chem. Soc.* **2005**, *127*, 7632–7637.

(51) Zhang, H.; Wang, G.; Chen, D.; Lv, X.; Li, J. Tuning Photoelectrochemical Performances of Ag−TiO_2 Nanocomposites via Reduction/Oxidation of Ag. *Chem. Mater.* **2008**, *20*, 6543–6549.

(52) Kazuma, E.; Tatsuma, T. In Situ Nanoimaging of Photoinduced Charge Separation at the Plasmonic Au Nanoparticle-TiO_2 Interface. *Adv. Mater. Interfaces* **2014**, *1*, 1400066.

(53) Murakoshi, K.; Tanaka, H.; Sawai, Y.; Nakato, Y. Photoinduced Structural Changes of Silver Nanoparticles on Glass Substrate in Solution under an Electric Field. *J. Phys. Chem. B* **2002**, *106*, 3041–3045.

(54) Naoi, K.; Ohko, Y.; Tatsuma, T. TiO_2 Films Loaded with Silver Nanoparticles: Control of Multicolor Photochromic Behavior. *J. Am. Chem. Soc.* **2004**, *126*, 3664–3668.

(55) Chung, S.; Choun, M.; Jeong, B.; Lee, J. K.; Lee, J. Atomic Layer Deposition of Ultrathin Layered TiO_2 on Pt/C Cathode Catalyst for Extended Durability in Polymer Electrolyte Fuel Cells. *J. Energy Chem.* **2016**, *25*, 258–264.

(56) Ghilane, J.; Fan, F.-R. F.; Bard, A. J.; Dunwoody, N. Facile Electrochemical Characterization of Core/Shell Nanoparticles. Ag Core/Ag_2O Shell Structures. *Nano Lett.* **2007**, *7*, 1406–1412.

TOC Graphic